Basolateral Protein Transport in Streptolysin O-permeabilized MDCK Cells

Sanjay W. Pimplikar, Elina Ikonen, and Kai Simons

Cell Biology Programme, European Molecular Biology Laboratory, Postfach 102209, 69012 Heidelberg, Germany

Abstract. We have reconstituted polarized protein transport in streptolysin O-permeabilized MDCK cells from the TGN to the basolateral surface and to the apical surface. These transport steps are dependent on temperature, energy and exogenously supplied cytosol. Using this in vitro system we show that a whole tail peptide (WT peptide) corresponding to the cytoplasmic tail of a basolaterally sorted protein, the vesicular stomatitis virus glycoprotein (VSV G) inhibits the TGN to basolateral transport but does not affect any other transport step. Inhibition of VSV G transport to basolateral surface by WT peptide did not result in missorting of the protein to the apical surface. Mutation of the single tyrosine residue in the WT peptide reduced its inhibitory potency four- to fivefold. These results suggest that the VSV G tail physically interacts with a component of the sorting machinery. Using a cross-linking approach, we have identified proteins that associate with the cytoplasmic tail domain of VSV G. One of these polypeptides, Tin-2 (Tail interacting protein-2), associates with VSV G in the TGN, the site of protein sorting, but not in the ER nor at the cell surface. Tin-2 does not associate with apically targeted hemagglutinin. WT peptide that inhibited the basolateral transport of VSV G also inhibited the association of Tin-2 with VSV G. Together, these properties make Tin-2 a candidate basolateral sorter. The results demonstrate the usefulness of the SLO-permeabilized cell system in dissecting the sorting machinery.

A hallmark of polarized epithelial cells is that their plasma membrane is divided into two domains, apical and basolateral, which are distinct in their lipid and protein composition. The newly synthesized apical and basolateral proteins occupy the same compartments while en route from the ER to the TGN which, in MDCK cells, is the site where they get sorted from each other (Rindler et al., 1984; Fuller et al., 1985; Griffiths and Simons, 1986). The sorted proteins are packaged in two distinct classes of vesicles (Wandinger-Ness et al., 1990) which are then targeted directly to the appropriate domains, thus bringing about the polarized delivery of proteins. In other cell types, some or all apical proteins are first delivered to the basolateral surface and then re-routed to their final destination by transcytosis (see Simons and Wandinger-Ness, 1990; Mostov et al., 1992; Rodriguez-Boulan and Powell, 1992). Beside a general appreciation of the pathways that apical and basolateral proteins follow to the cell surface, little is known about the molecular mechanisms that are responsible for the generation and maintenance of epithelial polarity.

To gain access to the molecular mechanisms, it is necessary to develop in vitro systems that allow experimental manipulation of molecules involved. The development of a cell-free assay to study intra-Golgi transport, together with genetic studies in yeast, has resulted in the identification of a number molecules involved in the process of vesicular transport (Rothman and Orci, 1992; Pryer et al., 1992). This approach of constructing in vitro assays has been successfully applied to study many other membrane trafficking events (reviewed in Pryer et al., 1992). There are basically two types of in vitro systems. Usually the assay consists of "donor" and "acceptor" compartments isolated from cell homogenates and monitors the transfer of a marker protein from the donor compartment to the acceptor (Balch et al., 1984; Gruenberg and Howell, 1989). The second approach aims at keeping these two compartments and most of the cellular architecture intact but introducing lesions in the cell membrane by mechanical (Simons and Virta, 1987) or chemical means (e.g., detergents or pore-forming toxins) and then monitoring the transfer of the marker protein between the two compartments (Gomperts, 1990; Gravotta et al., 1990; Tan et al., 1992). Both systems can be used to study effects of membrane impermeable reagents and macromolecules such as peptides and antibodies and have proved useful in identifying various protein components of the vesicular transport systems.

The observation that the apical as well as basolateral proteins when expressed in heterologous epithelial cells are largely routed to the correct domains suggests the presence

Address all correspondence to K. Simons, Cell Biology Programme, European Molecular Biology Laboratory, Postfach 102209, 69012 Heidelberg, Germany.

of common sorting machinery that recognize the sorting signals (reviewed in Rodriguez-Boulan and Powell, 1993). It is known that the glycosyl phosphatidyl inositol-anchored (GPI)[1] proteins are mostly delivered to the apical surface and that it is the GPI moiety that serves as the apical sorting determinant (Lisanti et al., 1988). With this exception, no other apical sorting signal has yet been identified. Recent studies have shown that cytoplasmic domains of several membrane proteins contain a basolateral sorting determinant (BSD). Initially shown to reside in the proximal 17 amino acids of the cytoplasmic tail of the polymeric immunoglobulin receptor (pIgR, Casanova et al., 1991), BSD's have now been located in the cytoplasmic tails of many basolateral proteins (Le Bivic et al., 1991; Hunziker et al., 1991; Yokode et al., 1992; Matter et al., 1992; Thomas et al., 1993; Prill et al., 1993). Some BSD's resemble closely the tyrosine-containing signals involved in rapid endocytosis from the cell surface. However, others are clearly different in structure. A typical BSD is usually contained in a 15–20-amino acid long peptide segment. The location of the BSD in the protein, normally close to the membrane spanning domain, seems critical for the activity of the signal (Le Bivic et al., 1991; Hunziker et al., 1991). The BSD's when genetically engineered into heterologous proteins seem capable of diverting an otherwise apical protein to the basolateral surface (Casanova et al., 1991). These properties strongly suggest that the BSD's interact with a specific basolateral sorting receptor (sorter) and mediate sorting of the protein into the basolateral vesicle.

We are interested in dissecting the sorting machinery and in identifying the individual molecules involved in the process of polarized sorting and targeting. Towards this goal, we have been developing an in vitro system capable of carrying out the multiple steps of polarized transport in MDCK cells. We make use of the bacterial toxin streptolysin O (SLO) to introduce pores selectively in either the apical or the basolateral surface and then monitor the appearance of vesicular stomatitis virus glycoprotein (VSV G) or influenza haemagglutinin (HA) at the intact surface. This approach was initially used by Gravotta et al. (1990) to study apical transport of HA in basolaterally permeabilized MDCK cells. We have previously reported conditions for obtaining cytosol-dependent apical transport of HA (Kobayashi et al., 1992; Pimplikar and Simons, 1993). Now we have achieved conditions to study cytosol-dependent basolateral transport of VSV G. The VSV G is preferentially routed to the basolateral surface in the permeabilized cells. Using this system, we provide evidence for the presence of the putative basolateral sorter and have identified a polypeptide that is likely to be part of the basolateral sorting machinery.

Materials and Methods

Cell Culture and Viral Infections

MDCK cells, strain II (low resistance) were cultured as described previously (Matlin et al., 1981). The cells from one confluent 75 cm^2 flask were suspended in 18 ml of growth medium (Eagle's minimal essential medium with Earle's salts [E-MEM] supplemented with 10 mM Hepes, pH 7.3, 10% (vol/vol) fetal calf serum, 100 U/ml penicillin, and 100 μg/ml streptomycin), and 1.5 ml of the cell suspension was seeded on each of 12 24-mm diam, 0.4-μm pore size Transwell™ polycarbonate filters (Costar, Cambridge, MA). The cells were used 3 d after plating by which time they displayed a transmonolayer electrical resistance of at least 150–200 Ω.cm^2.

The TGN to Basolateral Surface Transport. A stock of phenotypically mixed VSV (Indiana strain) grown in Chinese hamster ovary C15.CF1 cells which express HA on their plasma membrane was prepared as described (Bennett et al., 1988). Prior to viral infection, the monolayers were washed in warm infection medium (IM; E-MEM supplemented with 10 mM Hepes, pH 7.3, 0.2% (wt/vol) BSA, 100 U/ml penicillin, and 100 μg/ml streptomycin) and infected with 200 μl IM (50 pfu/cell; enough to obtain 100% infection as judged by immunofluorescence) on the apical side. After allowing adsorption of the virus to the cells for 1 h at 37°C, the inoculum was removed and the infection was continued for an additional 4 h after adding 1 ml IM on the apical and 2.6 ml IM on the basolateral side of the filter.

The TGN to Apical Surface Transport. Stock N Virus (A/chick/Germany/49/Hav2Neql) was grown in 11-d embryonated chicken eggs as described previously (Matlin and Simons, 1983). The cells were infected as described above with 10–20 pfu/cell except that following the 1-h adsorption period at 37°C the infection was continued for additional 3 h.

Pulse–Chase Experiments

The TGN to Cell Surface Transport. The cell monolayers were rinsed in beaker containing warm PBS+ (PBS containing 0.9 mM $CaCl_2$ and 0.5 mM $MgCl_2$) and pulse labeled in a wet chamber for 6 min at 37°C from the basolateral side with 100 μl of labeling medium (methionine-free E-MEM containing 0.35 g/l sodium bicarbonate (instead of the usual 2.2 g/l) and 10 mM Hepes, pH 7.3, 0.2% [wt/vol] BSA) containing 50 μCi of [^{35}S]methionine. The apical surface was covered with 400 μl of labeling medium. The pulse was terminated by washing the monolayers in chase medium (CM; labeling medium containing 40 μg/ml cycloheximide and 150 μg/ml cold methionine) and incubating for additional 6 min at 37°C. The filters were then transferred to fresh CM prewarmed to 19.5°C and further incubated at 19.5°C for 60–90 min to block the viral glycoproteins in the TGN (Matlin and Simons, 1984).

SLO Activation

The purified SLO (Bhakdi et al., 1984) was obtained from Dr. S. Bhakdi (University of Mainz, Mainz, Germany). Highly purified SLO preparations of various haemolytic titers were usually supplied in PBS+ containing 0.1% BSA. Each batch of the toxin was standardized for the amount of lactate dehydrogenase released from the filter-grown MDCK cells (see Results). The toxin was activated in KOAc buffer (115 mM KOAc, 25 mM Hepes, pH 7.4, 2.5 mM $MgCl_2$) containing 10 mM DTT at 37°C for 30 min and left at 4°C till used for permeabilization. The toxin was stored in aliquots at −70°C and activated toxin was used within 1 h of activation. The thawed aliquots of SLO were used once since the activity was rapidly lost upon repeated freeze–thawing.

Cell Permeabilization and Cytosol Depletion

The TGN to Basolateral Surface Transport. A two-step permeabilization protocol was followed. The monolayers were washed twice with KOAc+ buffer (KOAc buffer containing 0.9 mM $CaCl_2$ and 0.5 mM $MgCl_2$) at 4°C. The excess buffer from the apical side was carefully removed and activated SLO (enough to release 60% LDH in 30 min) in a volume of 50 μl was applied to the apical surface. After 13 min at 4°C, the apical surface was washed three times with ice-cold 1 ml KOAc+ buffer. The cytosol depletion was carried out at 19.5°C for 30 min by adding 1 ml transport medium (TM; 115 mM KOAc, 25 mM Hepes, pH 7.4, 2.5 mM $MgCl_2$, 1 mM DTT, 5 mM EGTA, and 2.5 mM $CaCO_3$) on the apical and 2 ml TM on the basolateral side of the filter.

The TGN to Apical Surface Transport. The permeabilization protocol was exactly as above except the activated SLO was applied from the basolateral side. It was observed that to get the same amount of LDH released from the basolateral side, approximately one third of the amount of SLO was needed compared to that used for apical permeabilization. In both these treatments no LDH was released from the nonpermeabilized surface.

1. *Abbreviations used in this paper*: BSD, basolateral sorting determinant; E-MEM, Eagle's minimal essential medium with Earle's salts; FPV, fowl plague virus; GPI, glycosyl phosphatidyl inositol-anchored; HA, influenza hemagglutinin; IM, infection medium; LDH, lactate dehydrogenase; pIgR, polymeric immunoglobulin receptor; SLO, streptolysin O; STI, soybean trypsin inhibitor; VSV G, vesicular stomatitis virus glycoprotein; WT, whole tail.

The TGN to Basolateral Surface Transport

VSV-infected MDCK monolayers were pulse-labeled, SLO permeabilized, and cytosol depleted as described above. After cytosol depletion the apical surface was gently rinsed once with TM and layered with 400 μl of TM or HeLa cytosol with or without ATP-regenerating system (1 mM ATP, 8 mM creatine phosphate, and 50 μg/ml creatine kinase). After 10 min at 4°C, the filters were placed on warm 100-μl drop of TM and incubated at 37°C for 45 min in a wet chamber. The transport was terminated by transferring the cells to 4°C and washing (three times) the monolayers with cold PBS+.

The amount of VSV G transported to the basolateral surface was measured by surface immunoprecipitation. All steps were performed at 4°C on ice. Following the PBS+ wash, the monolayers were washed once with antibody buffer (AB; E-MEM containing 0.35 g/l sodium bicarbonate [instead of the usual 2.2 g/l] and 10% [vol/vol] FCS). Antibodies raised against the luminal domain of VSV G protein (Pfeiffer et al., 1985) were affinity purified and 5 μl of antibodies were added to 70 μl of AB and the filters were placed on this 75-μl drop for 90 min. Nothing was added to the apical side. The excess unbound antibodies were removed over 30 min by three washes with AB and one wash with PBS+. The filters were gently shaken for the efficient removal of unbound antibodies. The monolayers were then incubated on a 75-μl drop of PBS+ containing excess cold virus to quench any unbound antibodies. The cells were then lysed on ice by adding 400 μl of lysis buffer (LB, PBS containing 2% NP-40 and 0.2% SDS) containing freshly added protease inhibitor cocktail (chymostatin, leupeptin, antipain, and pepstatin A; final concentration 25 μg/ml of each) and cold virus. The lysate was centrifuged in an Eppendorf microfuge for 5 min to remove insoluble material. At this stage the lysates were usually frozen in liquid nitrogen and stored overnight at −70°C. The lysates were thawed and centrifuged for 5 min to remove aggregates. A 20-μl aliquot was removed (total VSV G) and to the rest was added 50 μl of protein A–Sepharose (1:1) in LB. After shaking the mixture at 4°C for 60 min, the resin was washed (three times) with lysis buffer and the protein A bound (surface VSV G) was eluted by boiling with Laemmli sample buffer. Both the total and surface VSV G was analyzed by SDS-PAGE on a 10 % acrylamide gel (Laemmli, 1970). The band intensities were calculated using PhosphorImager (Molecular Dynamics, Sunnyvale, CA) and the amount of VSV G transported was calculated as the amount of VSV G bound to protein A–Sepharose after normalizing for recoveries. This and other transport assays were carried out routinely on duplicate filters at least twice and the quantifications represent the means of one representative experiment.

The TGN to Apical Surface Transport

N virus infected MDCK monolayers were pulse-labeled, SLO permeabilized and cytosol depleted as described above. After cytosol depletion the basolateral surface was gently rinsed once with TM and the filters were placed on a 100-μl drop of TM or HeLa cytosol as above. After 20 min at 4°C, the filters were layered with warm 400 μl of TM and incubated at 37°C for 45 min in a wet chamber. The transport was terminated by transferring the cells to 4°C and washing (three times) the monolayers with cold PBS+.

The amount of HA transported to the apical surface was measured with a modification in the trypsin cleavage protocol described earlier (Matlin and Simons, 1983). All steps were performed at 4°C on ice. Following the PBS+ wash, the apical surface received 500 μl of 200 μg/ml trypsin in PBS+ while to the basolateral chamber was added 750 μl of 100 μg/ml soybean trypsin inhibitor (STI) in PBS+. After 30 min of incubation, the reaction was stopped by adding 50 μl of STI (1 mg/ml) to the apical side and then by washing the apical surface twice with PBS+ containing 50 μg/ml STI. The monolayers were then solubilized in 500 μl LB as above and analyzed by SDS-PAGE on a 10% acrylamide gel. The band intensities were calculated using PhosphorImager and the amount of HA transported was calculated as described before (Matlin and Simons, 1983; percent of transport = 2 × HA2/HAO + 2HA2 × 100.

Transport to the Golgi: Endoglycosidase H Resistance Assay

VSV-infected MDCK monolayers were pulse-labeled for 10 min and then incubated for 30 min at 40°C before SLO permeabilization. The permeabilization protocol was exactly as used for the TGN to apical surface transport with the following modifications. After 13 min at 4°C, the unbound SLO was washed off from the basolateral side as above. The cytosol-depletion procedure was modified and was carried out at 37°C for 3 min with 1 ml TM on the apical and 2 ml TM on the basolateral side of the filter. This was followed by 4°C for 20 min in fresh TM. During the first incubation at 37°C for 3 min the pores were formed and ~30% LDH was released in the medium. During the second incubation 4°C for 20 min another 30–35% LDH was released. Thus, total LDH release was similar to that in the case of TGN to cell surface transport but this modification allowed the retention of the labeled viral glycoproteins in the ER. The transport was carried out exactly as described for the TGN to apical surface transport. The transport was terminated by transferring the cells to 4°C and washing (three times) the monolayers with cold PBS+. The monolayers were then solubilized in 500 μl of LB as above. After removing the unsolubilized material by centrifugation for 5 min, a 75-μl aliquot was removed and added to 25 μl of 0.2 M sodium citrate buffer, pH 5.0. The resulting 100-μl mixture had a pH 5.3 and was divided in two 50-μl aliquots. One received 5 μl of 1 U/ml endoglycosidase H (Seikagaku Kogyo Ltd., Tokyo, Japan) and the other received only citrate buffer. After 20 h at 37°C, the reaction was terminated by boiling in Laemmli sample buffer and the samples were analyzed by SDS-PAGE on a 10% acrylamide gel. The band intensities were calculated using PhosphorImager and the amount of HA transported was calculated as the percent of HA acquiring endoglycosidase H resistance.

Preparation of HeLa Cytosol

HeLa cells were grown in suspension to a density of 4–6 × 10^5/ml. Cells, in log growth phase, were harvested by centrifugation at 1,500 rpm in Beckman J-6B and the pellets were washed with ice cold PBS. Finally, the cells were suspended in swelling buffer (1 mM EGTA, 1 mM $MgCl_2$, 1 mM DTT, and 1 μM cytochalasin D) for 5 min on ice and centrifuged as above. As much supernatant as possible was removed and the cells were homogenized, after adding protease inhibitor cocktail, with a hand held all glass Dounce homogenizer with five strokes. To the homogenate was added 0.1 vol of 10X KOAc buffer and further homogenized with 10 strokes. By this procedure 70–80% of cells were broken as judged by light microscopy. The homogenate was centrifuged at 19,000 rpm for 10 min in SS-34 rotor followed by another centrifugation at 50,000 rpm for 90 min in Ti-70 rotor. The supernatant thus obtained was frozen in small aliquots stored frozen in liquid nitrogen. This procedure routinely yielded ~40 mls of 8–10 mg/ml cytosol from 16 l of cell suspension. When needed, the aliquots were quickly thawed and kept on ice till use.

Release of Transport Markers from Perforated Cells

MDCK strain II cells from one confluent 75-cm^2 flask were seeded on a 100-mm diam, 0.4-μm pore size Transwell filter as described previously (Wandinger-Ness et al., 1990) and the cultures maintained for 3 d. Viral infections with fowl plague virus (FPV/A/Rostock, Hav1 N1) or VSV (Indiana strain; see above) were performed according to Wandinger-Ness et al. (1990). The cells were rinsed in warm PBS+ and labeled at 37°C for 6 min from the basolateral side with 300 μl of labeling medium (see above) containing 250 μl [^{35}]methionine. The apical surface was covered with 1 ml of labeling medium. The pulse was terminated by incubating the cells in chase medium (see above) for additional 6 min at 37°C and the viral glycoproteins were accumulated in the TGN using a 60–90-min incubation at 19.5°C. The cell monolayer was then perforated with a nitrocellulose filter as described before (Wandinger-Ness et al., 1990). After perforation, 1-cm^2 squares were cut from the filter with a sharp scalpel and each piece transferred to a separate well of a 24-well dish containing either 250 μl KOAc-buffer with 2 mm EGTA and 1 mm DTT, or 250 μl Hela cytosol (8 mg protein/ml) with or without 25 μm whole tail (WT) peptide. In addition, +ATP samples contained an ATP regenerating system (see above) and −ATP samples an ATP depleting system (0.5 mg/ml hexokinase, 12.5 mM glucose). Cutting a large filter into pieces instead of using several smaller filters helped to standardize identical perforation of cells under each experimental condition. A moist Whatman filter was placed in the lid of the incubation chambers to minimize evaporation during the following 60-min incubation at 37°C. The incubation medium was collected, spun for 1 min in a microfuge, and a 10-μl aliquot from each incubation condition was resolved on a 10% SDS–polyacrylamide gel. The intensities of the HA2 and VSV G bands in each lane were calculated using PhosphorImager.

Chemical Cross-linking

A water-soluble and membrane-impermeable cross-linker (BS^3; Pierce Chemical Co., Rockford, Il) was used in these studies. A 10 mM stock solution of BS^3 was prepared in TM just prior to use. Filter-grown MDCK cells were permeabilized with SLO and the cross-linker (final concentration 1 mM) was added to cells from the permeabilized side. The reaction was

Table I. The Release of Cytosolic LDH with Increasing Concentrations of SLO

Amount of SLO	LDH released 15′	30′
μl	%	
2	0	2
5	5	20
10	31	55
25	53	67
50	57	70

Filter-grown MDCK cells were treated, in a final volume of 50 μl, with increasing amounts of SLO (hemolytic titer, ~1:3,000) on the apical side at 4°C. After removing the excess toxin, the cells were incubated at 19.5°C for 15 or 30 min and the amount of LDH released from the apical side was measured and expressed as percent of the total cellular LDH. No LDH was released from the basolateral side.

carried out usually at 37°C for 20 min and terminated by washing (three times) the monolayer with ice-cold PBS+ containing 50 mM Tris. The cells were lysed in 500 μl LB, VSV G (Pfeiffer et al., 1985) or HA (Matlin and Simons, 1984) were immunoprecipitated and analyzed by SDS-PAGE on 6% gel.

Analytical Techniques

VSV-G or influenza HA samples obtained after the transport reactions were analyzed by SDS-PAGE on a 10% acrylamide gel or (6% for the cross-linking experiments; Laemmli, 1970) and the gels were fluorographed using Entensify (Du Pont, New England Nuclear, Boston, MA). The dried gels were exposed to X-OMAT AR film (Eastman Kodak Co., Rochester, NY) at −70°C for 2–4 d. Protein assay was performed according to the Micro BCA protocol (Pierce Chemical Co.).

Results

SLO Permeabilization and Cytosol Dependence of the Transport Processes

The advantage of using SLO to permeabilize polarized cells is that pores can be selectively formed in one domain of the cell surface while keeping the other domain intact. When applied to a given surface at 4°C, SLO binds to cholesterol but does not form pores (Bhakdi and Tranum-Jensen, 1987). The unbound SLO can be washed away prior to raising the temperature which is necessary to induce pore formation. In this way pores are formed only on the surface exposed to SLO while the opposite domain and internal membranes remain intact. The efficacy of the permeabilization procedure was monitored by measuring the release of the cytosolic marker, lactate dehydrogenase (LDH). Table I shows that with increasing concentrations of SLO during the 4°C incubation, progressively more LDH was released upon raising the temperature. Maximum LDH release was around 70–80% and neither a higher amount of SLO nor an increased time of incubation released more LDH. To get the same amount of LDH released, the apical side required two to three times the amount of SLO needed for the basolateral domain (data not shown).

To make the transport steps dependent on exogenously added cytosol, the amount of SLO and the time of incubation used during cytosol depletion turned out to be crucial. Initial studies showed that the best results were obtained with the concentration of SLO that released around 60% LDH in 30

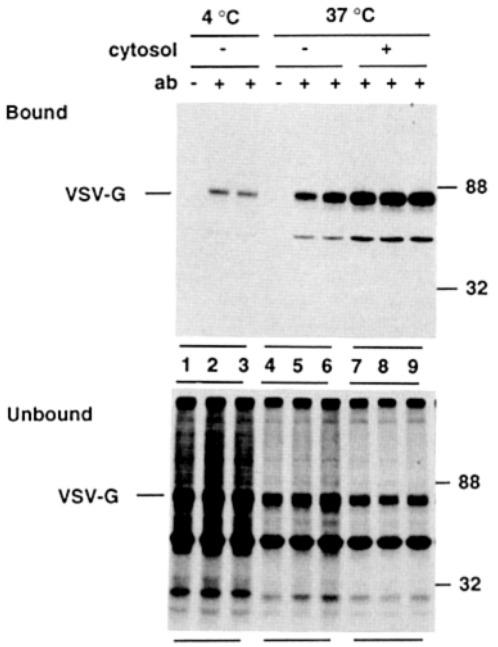

Figure 1. In vitro transport of VSV G from the TGN to basolateral surface is enhanced by exogenous addition of cytosol. Filter-grown MDCK cells were infected with VSV and the viral proteins were pulse-labeled with [^{35}S]methionine. After accumulating VSV G in the TGN the cells were permeabilized and the cytosol was depleted from the apical side. The cells were then left at 4°C (lanes *1–3*) or incubated for 45 min at 37°C in the absence (lanes *4–6*) or presence (lanes *7–9*) of exogenously added cytosol. The transport was terminated by cooling the cells to 4°C and VSV G protein was surface immunoprecipitated by adding antibodies on the intact basolateral surface. The cells were lysed, immunoprecipitates were collected on protein A–Sepharose and analyzed by SDS-PAGE. Lanes *1* and *4* show control immunoprecipitations performed in the absence of antibodies. (*Top*) Protein A–bound material; (*bottom*) one tenth of the unbound material. This and other transport assays were carried out on duplicate or triplicate filters and the experiments were performed at least twice. Values from various experiments (n = 6) for percent of VSV G transported to cell surface at 4°C, 11.5, S.D. 4.98; without cytosol, 21.9, S.D. 5.05; and with cytosol, 42.4, S.D. 1.72.

min at 19.5°C. When higher concentrations of SLO or increased time of incubation were applied to get as much cytosol depletion as possible (80% LDH release) we found that the transport activity was lost. With mild cytosol depletion (<50% LDH release), the signal caused by the addition of cytosol was not much higher than that obtained with the remaining endogenous cytosol. Thus, there was a narrow window of SLO concentration and cytosol-depletion conditions which gave the best results. At this level of SLO no detectable LDH was released from the opposite domain and 100% of the cells were permeabilized as judged by immunofluorescence studies (data not shown). The purity of SLO was of crucial importance. We used chromatographically purified SLO (a kind gift from Dr. S. Bhakdi, University of Mainz, Mainz, Germany). Commercial sources of SLO could not be used to obtain cytosol-dependent transport (data not shown).

Fig. 1 shows that appearance of VSV G on the basolateral surface was significantly stimulated upon addition of cyto-

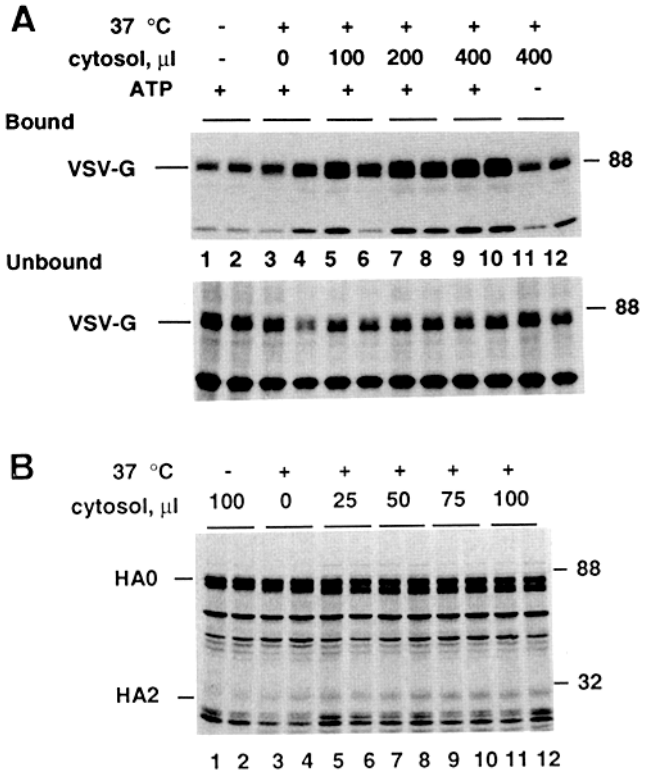

Figure 2. Cytosol dependence of the polarized transport processes. (*A*) In vitro transport of VSV G from the TGN to basolateral surface was carried out as described in Fig. 1 *A* except that increasing amounts of cytosol were added in a total volume of 400 µl from the permeabilized apical side. (*B*) In vitro transport of HA from the TGN to apical surface. Filter-grown MDCK cells were infected with influenza N virus and the pulse-labeled HA was accumulated in the TGN. The cells were permeabilized and the cytosol was depleted from the basolateral side. The transport was carried out for 45 min with increasing amounts of cytosol in a total volume of 100 µl. To assess the extent of transport, the cells were trypsinized from the intact apical side and the samples were analyzed by SDS-PAGE.

sol. There was no signal when the surface immunoprecipitation was carried out in the absence of antibodies (Fig. 1, lanes *1* and *4*). The cells left at 4°C gave a low background signal due to VSV G that had already reached the surface prior to the transport reaction (Fig. 1, lanes *2* and *3*). Upon addition of an ATP-regenerating system and raising the temperature to 37°C, slightly more protein reached the surface (Fig. 1, lanes *5* and *6*). This was probably due to the endogenous cytosol that was not removed during the cytosol depletion. However, after the addition of cytosol much more VSV G reached the basolateral surface (Fig. 1, lanes *7–9*).

Usually, 10–15% of the marker protein is found at the surface at the beginning of the transport assay due to the leakiness of the "20°C block". When the transport assay is performed in the absence of added cytosol (but in the presence of ATP) ~15–20% of protein is found at the surface. In the presence of cytosol up to 40–45% of protein is found at the surface which is completely abolished in the presence of ATP depleting system (see Fig. 2 *A*). The intact cells under same conditions transport 70–75% of viral proteins to the cell surface showing that the extent of transport in permeabilized cells is around 50% of the intact cells. Thus, typically 20–25% of the viral protein transported to the cell surface in the in vitro assay is dependent on exogenously added cytosol.

Fig. 2 *A* shows that there was a linear increase in the amount of VSV G transported from the TGN to basolateral surface when an increasing amount of cytosol was used in the assay (Fig. 2 *A*, lanes *1–10*) and that the transport was dependent on the supply of ATP (lanes *11* and *12*). Similarly, the transport of HA from the TGN to apical surface (Fig. 2 *B*) showed similar dependence on the amount of cytosol used in the assays. Thus, in SLO permeabilized, filter-grown MDCK cells these two steps of membrane transport are temperature and energy dependent and require exogenously added cytosol. We used Hela cytosol for the experiments documented here. However, MDCK cytosol would work just as well (data not shown).

A Peptide Corresponding to the Cytoplasmic Tail of VSV G Selectively Inhibits Basolateral Delivery of the Protein

Many basolateral membrane proteins, including VSV G, are known to carry a BSD in their cytoplasmic domains. A recent study has shown that when the cytoplasmic tail of HA was replaced with that of VSV G, the chimeric protein was diverted to the basolateral surface (Thomas et al., 1993) suggesting that the VSV G tail may interact with the sorting machinery. If this were true, then one would expect that a peptide corresponding to the VSV G tail will compete for this interaction and this should result in the inhibition of basolateral transport of VSV G. To test this prediction a peptide corresponding to the whole tail of VSV G (WT peptide; amino acid sequence in single letter code RVGIHLCIKLKHTKKRQIYTDIEMNRLGK) was introduced in permeabilized cells together with cytosol. Fig. 3 *A* shows that with increasing amounts of the peptide, less VSV G was delivered to the surface. The concentration of peptide needed to get 50% inhibition was in the range of 15–20 µM (Fig. 3 *B*). By contrast, addition of the peptide to cytosol did not affect the TGN to apical transport to any significant extent (Fig. 3 *C*). We also tested whether the WT peptide would inhibit transport of VSV G to the Golgi. It is known that the sorting of apical and basolateral proteins does not take place at this stage but later in the TGN. If the inhibition of basolateral transport by the WT peptide were specific to events occurring in the TGN then one would not expect the peptide to affect the transport of VSV G in the early part of the biosynthetic pathway. Fig. 3 *D* shows that the acquisition of endoglycosidase H resistance by VSV G was not affected in the presence of increasing amounts of WT peptide.

Specificity of the inhibition of basolateral transport by the peptide was further confirmed by constructing a point mutation in the WT peptide. Many BSD's are critically dependent upon the presence of a tyrosine residue for proper functioning. It has been suggested that the single tyrosine residue (tyrosine 501) in the VSV G tail is important for the basolateral delivery of the protein (Thomas et al., 1993). To test this, the tyrosine residue in the WT peptide was replaced with an alanine residue and the mutant peptide (WT-A peptide; amino acid sequence in a single letter code RVGIHLCIKLKHTKKRQIATDIEMNRLGK) was tested for its in-

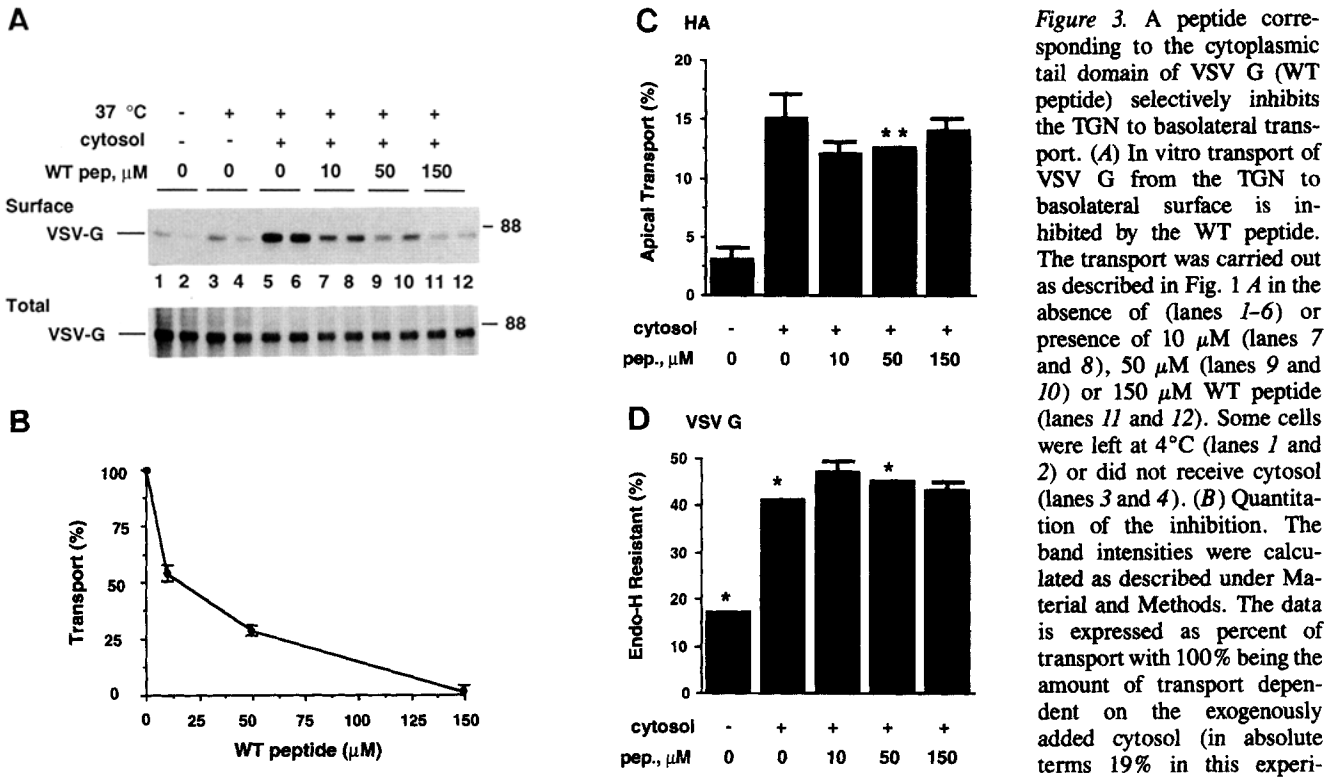

Figure 3. A peptide corresponding to the cytoplasmic tail domain of VSV G (WT peptide) selectively inhibits the TGN to basolateral transport. (*A*) In vitro transport of VSV G from the TGN to basolateral surface is inhibited by the WT peptide. The transport was carried out as described in Fig. 1 *A* in the absence of (lanes *1–6*) or presence of 10 μM (lanes *7* and *8*), 50 μM (lanes *9* and *10*) or 150 μM WT peptide (lanes *11* and *12*). Some cells were left at 4°C (lanes *1* and *2*) or did not receive cytosol (lanes *3* and *4*). (*B*) Quantitation of the inhibition. The band intensities were calculated as described under Material and Methods. The data is expressed as percent of transport with 100% being the amount of transport dependent on the exogenously added cytosol (in absolute terms 19% in this experiment). The values represent the mean of duplicate filters and the bars indicate the variation from the mean. (*C* and *D*) The WT peptide does not inhibit the TGN to apical transport of HA (*C*), or transport of VSV G to Golgi (*D*). The transport assays and quantitations were performed as described under Materials and Methods. Each column represents the mean of two filters and the bars indicate the variation from the mean; *, the variation between the duplicate values was less than 2; **, single determination.

hibitory activity on the basolateral transport of VSV G. At low concentration (15 μM) only the WT peptide (Fig. 4 *A*; compare lanes *3* and *4* vs. *5* and *6*) and not the WT-A peptide was inhibitory (lanes *9* and *10*), though at high concentration (150 μM) both peptides inhibited the transport (lanes *7* and *8*, *11* and *12*). Fig. 4 *B* shows that with increasing amounts of WT-A peptide the inhibition of transport was seen only at high concentrations. In order to get 50% inhibition of transport ~80–90 μM of the WT-A peptide was needed as opposed to 15–20 μM of the WT peptide. We then tested the ability of a peptide corresponding to the last 15 amino acids of the VSV G tail (called Y peptide since it contains the tyrosine residue proposed to be important for the functioning of the signal (see Thomas et al., 1993; the sequence in one letter code, KRQIYTDIEMNRLGK) to block transport. This peptide showed no or only mild inhibition of basolateral transport of VSV G (data not shown). We finally studied the effect of the peptide corresponding to the BSD of pIgR (the sequence in one letter code RARHRRNVDRVSIGSYR) and several mutant peptides containing alanine substitutions (both the wild type and the mutant peptides were kindly provided by B. Aroeti and K. Mostov, UCSF, San Francisco, CA). These peptides also failed to inhibit the basolateral transport of VSV G (data not shown).

VSV G Is Not Missorted to the Apical Surface in the Presence of WT Peptide

These data show that the WT peptide specifically prevents VSV G from arriving at the basolateral surface possibly by interfering with the interaction of VSV G tail and the basolateral sorting protein in the TGN. Would this interference result in missorting of VSV G to the apical surface? To answer this question, VSV-infected MDCK cells were permeabilized from the basolateral side and the amount of VSV G appearing at the intact apical surface was monitored in the presence of increasing amounts of the WT peptide. Fig. 5 *A* shows that the amount of VSV G appearing at the apical surface in the control cells (lanes *3* and *4*) was exceedingly small as compared with that appearing at the basolateral surface (for example, compare with Fig. 3 *A*). After normalizing for the amount of sample loaded on the gel and the time of exposure to get comparable intensities, roughly 15–20 times more VSV G is found at the basolateral surface as compared to the apical surface. This shows that the permeabilized MDCK cells exhibit the same correct sorting behavior as intact MDCK cells. Moreover, the amount of VSV G appearing at the apical surface did not show any consistent significant change when the transport was carried out in the presence of increasing amounts of WT peptide (Fig. 5 *A*, lanes *5–10*). Fig. 5 *B* shows the quantitation from two such experiments. Thus, it seems that the inhibition of VSV G transport to the basolateral surface does not result in significant missorting of the protein to the "wrong" surface.

Formation of Basolateral Transport Vesicles Containing VSV G Is Inhibited by WT Peptide

Our assay for transport from the TGN to the plasma membrane domains measures surface delivery. In order to find

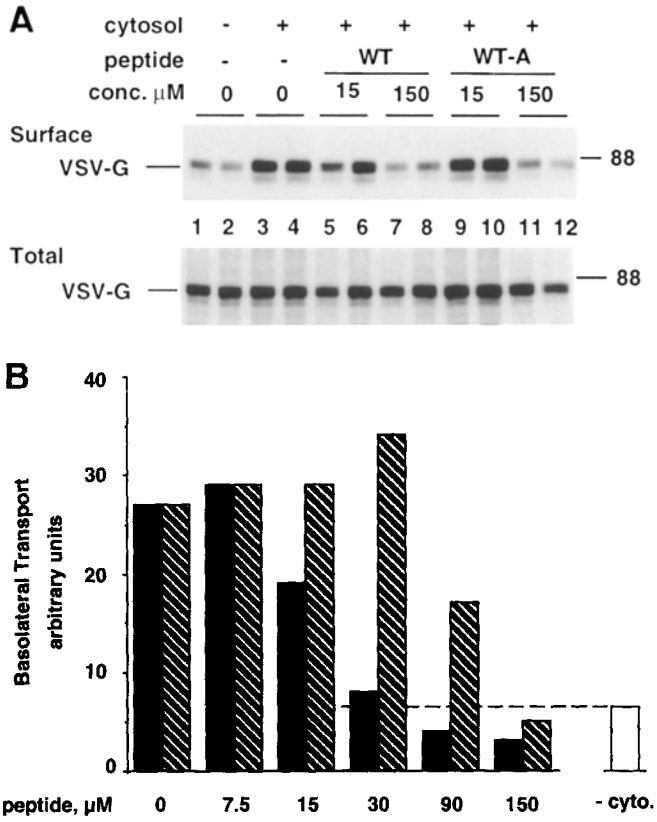

Figure 4. The inhibition of the basolateral transport by the WT peptide is dependent on the presence of a tyrosine residue. (*A*) A mutant WT peptide (*WT-A*) that carries an alanine residue in place of the tyrosine does not inhibit in vitro transport of VSV G from the TGN to basolateral surface at low concentrations. The transport was carried out as described in Fig. 1 *A* in the absence of (lanes *1–4*) or presence of 15 μM (lanes *5, 6, 9,* and *10*) or 150 μM (lanes *7, 8, 11,* and *12*) WT peptide (lanes *5–8*) or WT-A peptide (lanes *9–12*). Some cells did not receive cytosol (lanes *1* and *2*). (*B*) Quantitation of the inhibition. The in vitro transport assay was carried in the presence of increasing amounts of either WT (*filled columns*) or WT-A peptide (*hatched columns*). The band intensities were calculated as described under Materials and Methods. The values for the transport performed in the absence of cytosol (*open column*) and that performed in the presence of 0, 15, and 150 μM of both WT and WT-A peptides represent the quantitation of the gel shown in *A*. The values represent the mean of duplicate filters and the variation between the duplicate values was in the similar range as that in Fig. 3. The dashed horizontal line shows the extent of transport in the absence of exogenously added cytosol.

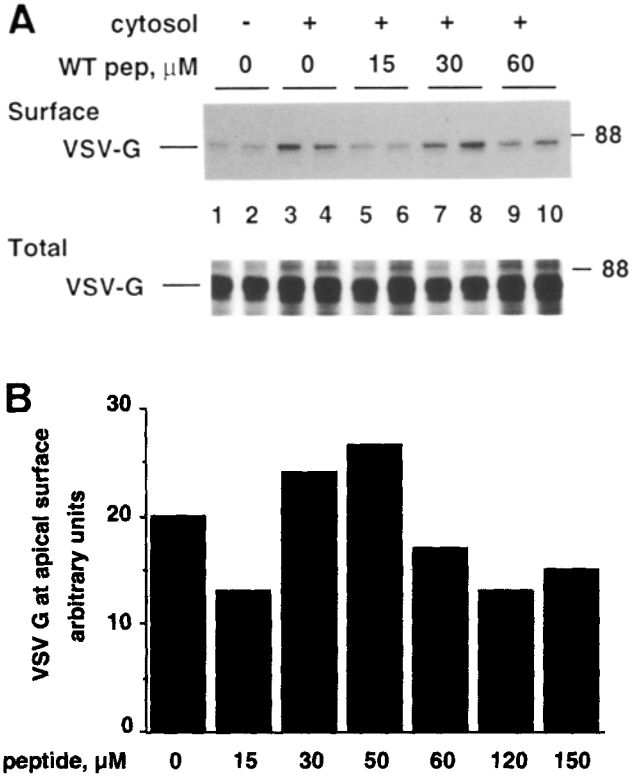

Figure 5. The inhibition of the basolateral transport by the WT peptide does not result in the missorting of VSV G to the apical surface. (*A*) The in vitro transport reaction was performed on VSV-infected cells as described in Fig. 1 *A* except that the cells were permeabilized from the basolateral side and the appearence of VSV G at apical surface was monitored by surface immunoprecipitation. The transport was carried out in the absence of (lanes *1–4*) or presence of 15 μM (lanes *5* and *6*), 30 μM (lanes *7* and *8*) or 60 μM WT peptide (lanes *9* and *10*). Some cells did not receive cytosol (lanes *1* and *2*). Aliquots from the Surface and Total were loaded in the same proportions as for the usual basolateral transport but the top gel (*Surface*) was exposed three times longer than the bottom gel (*Total*). (*B*) Quantitation of the inhibition. The in vitro transport assay was carried in the presence of varying amounts of the WT peptide and the band intensities were calculated as described under Materials and Methods. The values for the VSV G appearing at the apical surface in the presence of 0, 15, 30, and 60 μM of WT peptide represent the quantitation of the gel shown in *A*. The values represent the mean of duplicate filters. Note that in absolute terms, these values are 15–20 times lower than that found on the basolateral surface (for example see Fig. 2 *A*).

out whether or not the WT peptide blocks the formation of basolateral vesicles containing VSV G in the TGN we used perforated MDCK cell layers. Using nitrocellulose-perforated cells we have previously demonstrated that apical and basolateral transport vesicles can be released to the extracellular medium under appropriate conditions (Bennett et al., 1988). The exit of the vesicular markers, cleaved FPV HA (HA2) and VSV G, from the TGN was shown to be temperature and ATP dependent. We have now found that using exogenous cytosol instead of a buffer in the system resulted in two- to threefold stimulation of vesicle release. When the perforated cells were incubated with 25 μM WT peptide under conditions promoting maximal vesicle release (at 37°C in the presence of an ATP regenerating system and cytosol), the formation of VSV G containing vesicles was inhibited by 50% (Fig. 6 *A*). However, the WT peptide had no effect on the release of FPV HA2 (Fig. 6 *B*).

Different Polypeptides Associate with the Cytoplasmic Tail of VSV G during Its Passage to the Cell Surface

Our data suggest that the inhibition of basolateral transport of VSV G by the WT peptide is taking place at the stage of basolateral vesicle formation. This would imply that the VSV G tail is recognized by a putative basolateral sorter protein in the TGN and that the WT peptide interferes with this

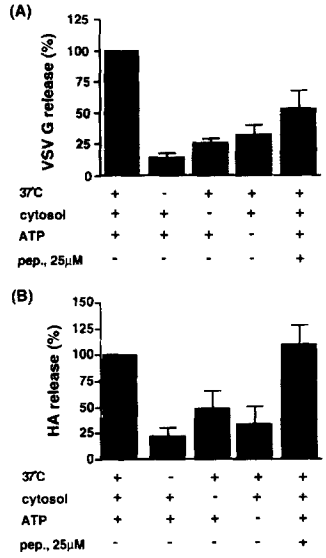

Figure 6. The WT peptide inhibits the release of VSV G (*A*) but not that of FPV HA2 (*B*) from perforated cells. Filter cultures were infected with VSV (*A*) or FPV (*B*), pulse labeled with [^{35}S]methionine and the viral proteins accumulated in the TGN as detailed in Materials and Methods. The cells were perforated and equal sized squares were cut from the cell filter. The filter pieces were incubated at 37° or 4°C for 60 min either in the presence or absence of cytosol, ATP, and WT peptide as indicated. Aliquots of the incubation medium were analyzed by SDS-PAGE and the intensities of VSV G and HA2 bands quantitated. The data is expressed as percent VSV G or HA2 release with 100% being the amount of marker released at 37°C in the presence of cytosol and ATP and 0% the amount released at 4°C in the absence of cytosol and ATP. Each column represents the mean of values obtained from five (*A*) and three (*B*) filter pieces and the bars indicate the standard deviation.

interaction. The putative sorter protein should exhibit at least two characteristic properties. It should interact with VSV G on the cytoplasmic and not on the luminal side and the interaction should take place in the TGN and not in the ER or at the cell surface. In order to detect this association, we developed a strategy of "compartment selective" cross-linking. MDCK cells were infected with VSV and the pulse-labeled VSV G protein was accumulated at different locations by incubating the cells for 90 min at 4°C (ER), 19.5°C (TGN), or 37°C (plasma membrane). The cells were permeabilized and a water-soluble, membrane-impermeable chemical cross-linker (Staros, 1982) was introduced immediately after SLO permeabilization. Under these conditions the cross-linking should occur only on the cytoplasmic side and only those proteins which associate with the tail of VSV G should be cross-linked to the viral protein. The cells were then lysed and VSV G was immunoprecipitated with an antibody raised against the luminal domain of the protein. Any cross-linking event will result in an upward shift of the VSV G band on SDS-PAGE analysis. In the absence of the cross-linker, there was only one major band of VSV G and a minor band at ~150 kD (Fig. 7 *A*, lanes *1*, *4*, and *7*). When cross-linked, VSV G blocked in the ER showed a new cross-linked band at ~100 kD and was termed Tail interacting protein-1 (Tin-1; Fig. 7 *A*, lanes *2* and *3*). When VSV G was accumulated in the TGN, two bands were seen on the gel; Tin-1 and Tin-2 at ~300 kD (Fig. 7 *A*, lanes *5* and *6*). When VSV G protein reached the plasma membrane Tin-2 disappeared and only Tin-1 with two new bands, Tin-3 (at ~180 kD) and Tin-4 (at ~250 kD) appeared in the gel (Fig. 7 *A*, lanes *8* and *9*). Some of the faint minor bands seen upon cross-linking disappeared when the cross-linking was performed on cytosol-depleted cells (see Fig. 7 *D*). Further, both Tin-1 and Tin-2 were completely absent when the cross-linker was added to intact cells (data not shown).

Thus, Tin-1 associates with VSV G already in the ER but seems associated at later stages as well. Tin-2 seems to associate with VSV G only in the TGN. A faint smear of Tin-2 sometimes seen in the ER samples (Fig. 7 *A*, lane *2*) is due to the fact that cross-linking was performed at 37°C and during the reaction some of the protein might escape to the TGN. When the cross-linking was performed at 4°C instead of 37°C, Tin-2 appeared in the TGN (Fig. 7 *B*, lanes *3* and *4*) and not in the ER (lanes *1* and *2*). However, the efficiency of cross-linking is low at 4°C compared to that at 37°C and so the reaction is routinely performed at 37°C for 20 min. Tin-3 and Tin-4 appeared only after VSV G had arrived at the cell surface (Fig. 7 *A*). The 150-kD band was sometimes present in the non cross-linked samples but appeared strongly after cross-linking. For a number of reasons, its status is not clear (see Discussion).

If Tin-2 is important for basolateral sorting of the VSV G protein, one would not expect it to associate with an apically targeted protein. Therefore, an analogous experiment was performed to see whether Tin's or other proteins associate with HA via the latter's cytoplasmic tail. MDCK cells were infected with influenza virus and the pulse-labeled HA protein was accumulated at different locations. Fig. 7 *C* shows that ER-accumulated HA, upon cross-linking, yielded a number of extra bands (lanes *3* and *4*) which were not present when cross-linker was not added to the cells (lane *2*) or when the cells were not permeabilized to prevent the entry of the cross-linker (lane *1*). The same set of bands were present when the HA was chased either to the TGN (Fig. 7 *C*, lanes *7* and *8*) or to the plasma membrane (lanes *11* and *12*). No new bands were observed in these two locations and no band was observed in the region of Tin-2. Since VSV G and HA have approximately the same mobility on the SDS-PAGE gels, it can be concluded that Tin-2 does not associate with HA.

Since the WT peptide blocked the basolateral transport of VSV G, we studied the effect of peptide on the association of Tin-2 with VSV G. The cross-linking experiment was slightly modified. Pulse-labeled VSV G protein was accumulated in the TGN. The cells were permeabilized with SLO and the cytosol was depleted. The peptide was then added to cells in buffer alone and allowed to pre-incubate with the cells for 30 min prior to the addition of the cross-linker. Under these conditions the WT peptide significantly inhibited appearance of Tin-1 and Tin-2 without affecting the appearance of the 150-kD protein. The degree of inhibition was dependent on the concentration of peptide (Fig. 7 *D*). Using 150 μM WT peptide the intensities of Tin-1 and Tin-2 bands were reduced by 80 and 50%, respectively. It is not surprising that we do not observe complete inhibition of VSV G-Tin-2 interaction. At the time the peptides are added to the cells, VSV G in the TGN is probably already associated with Tin-2 and this necessitates the use of higher concentrations of peptides (we routinely use 150 μM WT peptide) to achieve consistently significant inhibition of Tin-2 interaction. Inhibition of cross-linking of Tin to VSV G in the presence of WT peptide cannot be due to the peptide blocking the cross-linker by reacting through their free amino groups since the cross-linking reagent is used in vast excess (1 mM). Also, the cross-linking of the 150-kD protein remained unaffected under these conditions (Fig. 7 *D*). Since the cross-linker is incapable of penetrating the membrane and since the WT pep-

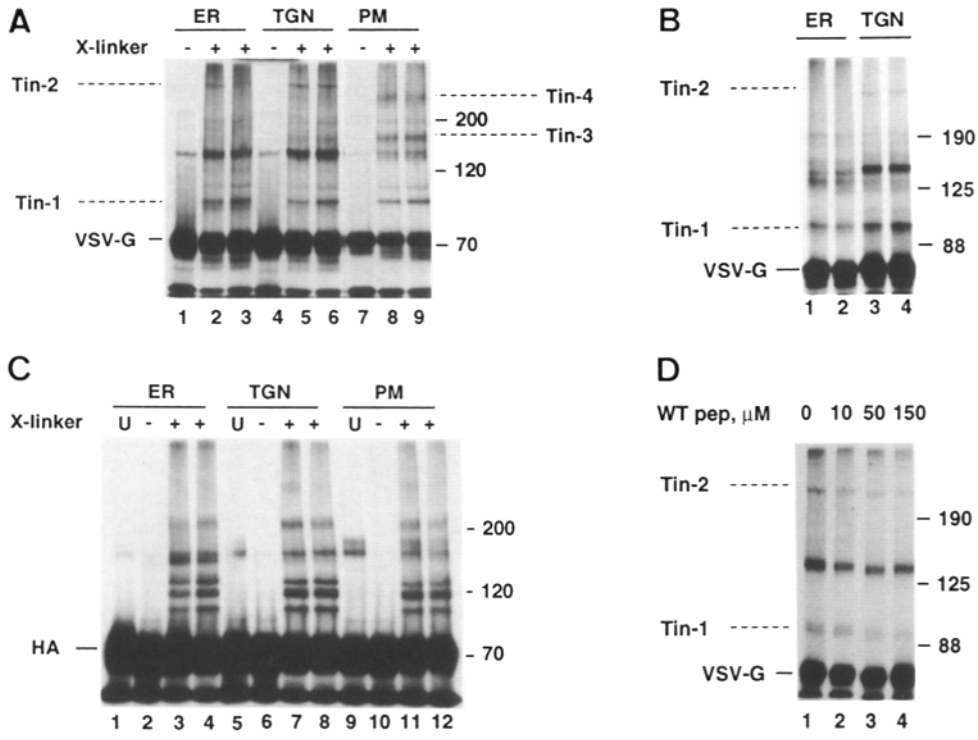

Figure 7. Different polypeptides can be cross-linked with the cytoplasmic tail of VSV G during its passage to the cell surface. (*A*) Filter-grown MDCK cells were infected with VSV and the pulse-labeled VSV G protein was accumulated in ER (lanes *1–3*), in the TGN (lanes *4–6*) or at the plasma membrane (lanes *7–9*) by incubating the cells for 90 min at 4°, 19.5°, or at 37°C, respectively. The cells were treated with SLO at 4°C from the apical side and BS^3 (final concentration 1 mM) was not added (lanes *1*, *4*, and *7*) or added (lanes *2*, *3*, *5*, and *6*) immediately upon raising the temperature to 37°C for 20 min. The cells were lysed and VSV G was immunoprecipitated with an antibody raised against the luminal domain of VSV G and analyzed by SDS-PAGE. (*B*) Filter-grown MDCK cells were infected with VSV and the pulse-labeled VSV G protein was accumulated in ER (lanes *1* and *2*) or in the TGN (lanes *3* and *4*) by incubating the cells for 75 min at 4°C or 19.5°C, respectively. The cells were treated with SLO at 4°C from the apical side, the cells were permeabilized by raising the temperature to 37°C for 3 min followed by incubation at 4°C for 20 min and the cross-linking was performed at 4°C (instead of 37°C) for 20 min. Note the complete absence of Tin-2 in the ER samples and the slightly higher mobility of the ER form of VSV G. Also note the absence of minor background bands due to leakage of cytosol; compare lanes *5* and *6* of *A* with lanes *3* and *4* of *B*. (*C*) The experiment was performed as described in *A* except that the cells were infected with influenza N virus. After accumulating the pulse- labeled HA in ER (lanes *1–4*), in the TGN (lanes *5–8*) or at the plasma membrane (lanes *9–12*), the cells were left unpermeabilized (lanes *1*, *5*, and *9*) or treated with SLO at 4°C from the basolateral side. HA was immunoprecipitated from the cell lysates with a polyclonal antibody raised against the luminal domain of the protein and analyzed by SDS-PAGE. (*D*) The experiment was performed as described in *A* except that after accumulating the pulse-labeled VSV G in the TGN and permeabilizing the cells, the cytosol was depleted from the apical side. The cells were then pre-incubated for 10 min at 4°C with increasing concentrations of WT peptide. BS^3 (final concentration 1 mM) was added upon raising the temperature to 37°C for 20 min. The WT peptide inhibits cross-linking of Tin-2 to VSV G. Note also that upon cytosol depletion many minor bands disappear following cross-linking (compare with *A*).

tide inhibits association of both Tin-1 and Tin-2, the results strongly suggest that the association of Tin's with the viral protein is mediated via the cytoplasmic tail of the VSV G.

Discussion

The aim of the present report is twofold. Firstly, we describe an in vitro system in which multiple steps of polarized protein transport can be studied in a cytosol-dependent manner. Secondly, we show the usefulness of the system by providing evidence that the basolateral sorting involves physical association of the BSD's with a putative sorter protein and by identifying a protein which could be involved in this process.

The SLO-permeabilized Cell System to Study Membrane Traffic

A complex process such as epithelial protein sorting can only be studied in an in vitro membrane transport system that maintains most of the cellular structure intact. This is not possible in the usual "acceptor- and donor-organelle" approach. By making use of SLO, a bacterial toxin, to selectively permeabilize either the apical or the basolateral domain of MDCK cell surface we have been able to construct assays that monitor transport from the TGN to both the apical and the basolateral plasma membrane domains. In this experimental system the process of polarized sorting of proteins to both cell surfaces can be studied for the first time in a cytosol dependent manner. Importantly, the SLO-permeabilized cells exhibit the same sorting behavior as in vivo.

Although several in vitro systems have been described based on the use of SLO (Gravotta et al., 1990; Tan et al., 1992), it was usually not possible to make the desired transport step solely or largely dependent on exogenously added cytosol. Our initial attempts at achieving such conditions gave irreproducible results. In trying to make the transport steps dependent on externally added cytosol, we found that the purity of SLO and the conditions used for cytosol depletion were crucial. Maximum cytosol depletion was deleterious to subsequent functioning of the cells while cells depleted of cytosol under gentle conditions still maintained structurally distinct intracellular organelles and responded

reproducibly to the addition of cytosol. To get an optimal transport signal the protein concentration in the externally added cytosol needs to be at least 8 mg/ml. We have successfully used cytosols prepared from MDCK cells, HeLa cells, and Xenopus oocytes though HeLa cytosol is routinely used because of the ease of preparation and the consistent results. The cytosol-depleted cells maintained tight junctions and the permeability barrier of intracellular membranes remained intact (Kobayashi et al., 1992). This proved to be of critical importance in the cross-linking experiments.

The Role of the VSV G Tail in Basolateral Transport

During the past years it has become evident that the transport of basolateral membrane proteins to their destination is a signal-mediated event. The nature and the location of BSD's suggested, but did not prove, that they functioned by physically interacting with sorter proteins. Two important findings of the present studies are that the basolateral transport of VSV G can be competed by adding the WT peptide and that the site of inhibitory action is at the stage of vesicle formation. These data suggest that basolateral protein sorting must be mediated by physical association with a protein, the putative sorter. The peptide does not inhibit the TGN to apical destiny of HA. This rules out nonspecific inhibitory effects of the peptide on membrane transport. Though the VSV G tail is shown to contain the BSD, the latter has not been precisely mapped to a specific part of the tail. The failure of the Y peptide (corresponding to distal 15 amino acids of the tail) to inhibit basolateral transport suggests that the sorting determinant extends upstream of the 15 amino acids or that the Y peptide simply fails to form the correct conformation. In any case, the importance of the tyrosine residue for the basolateral delivery of VSV G is confirmed by our studies. The WT peptide bearing an alanine instead of the tyrosine (WT-A peptide) is four to five times less effective in inhibiting the basolateral transport of VSV G. However, inhibition by the WT-A at higher concentrations in combination with the fact that 64% of VSV G is still delivered to basolateral domain in the absence of tyrosine 501 (Thomas et al., 1993) suggests the tyrosine residue is not essential for basolateral sorting (see also Prill et al., 1993). Thus, we have now extended the earlier observations that the single tyrosine residue (tyrosine 501) in the VSV G tail is important for the functioning of the signal (Thomas et al., 1993).

The lack of inhibition of VSV G transport by a peptide corresponding to the BSD of pIgR would suggest that the pIgR-BSD does not compete with the VSV G-BSD for the sorting machinery. In fact, there is no discernible sequence homology between these two or other known BSD's (however, they may form similar secondary structures). Either the pIgR peptides may compete poorly with VSV G for the sorting machinery or they may fail to achieve the right conformation. Alternatively, keeping the diversity of the BSD's in mind, it is possible that there is more than one basolateral sorter serving more than one basolateral route. The possibility that there may be more than one basolateral route was suggested earlier to account for the differential activity of two BSD's of the LDL receptor (Matter et al., 1992) and to explain the differential effects of brefeldin A on the basolateral transport of proteins (Apodaca et al., 1991).

The Tin's

Inhibition of the transport by the WT peptide strongly argues for the presence of sorter proteins which must bind to the VSV G tail in the TGN. Indeed, by introducing a membrane impermeable cross-linker into the permeabilized cells we have identified four polypeptides that associate with the VSV G tail at different stages of the exocytic pathway. Various controls indicate that the Tin's interact with the cytoplasmic domain and not with the luminal domain of the viral protein. The status of the 150-kD band is unclear for the following reasons: (*a*) it was sometimes seen in the noncross-linked samples; (*b*) when cross-linked with the thiol cleavable cross-linker DTSSP, this band was present even after reduction whereas the Tin's had disappeared (Pimplikar, S. W., unpublished data); (*c*) it could be cross-linked in the intact cells; and (*d*) the cross-linking was not competed by the WT peptide. The molecular weight of the 150-kD band suggests that this band could be a dimer of VSV G protein which, although known to exist as a trimer, has been shown to form transient disulfide-linked dimers in the ER (Kreis and Lodish, 1986). However, the possibility that 150-kD band represents a protein which could be important in membrane trafficking of VSV G can not be ruled out at the present moment.

Tin-1 appears to be the first protein to associate with the VSV G tail on its biosynthetic route and the association seems to persist as the viral protein continues its journey towards the final destination. Since it is difficult to chase the viral glycoproteins completely out of the ER, it is possible that Tin-1 seen associated with VSV G at the later stages is, in fact, due to VSV G remaining behind in the ER. The calculated molecular weight of Tin-1 (after subtracting the molecular weight of VSV G from that of the cross-linked product) is ~30 kD. The molecular identity of Tin-1 and its physiological relevance is currently unknown. Tin-1 is unlikely to be involved in the transport of VSV G from the ER to Golgi since the WT peptide disrupted its association with VSV G without affecting the transport. We have not tested the possibility that Tin-1 is the viral matrix protein M, which has a similar molecular weight.

Tin-2 associates with the VSV G tail only in the TGN and this association is lost as the VSV G reaches the cell surface. Its calculated molecular weight is in the range of 200–230 kD. There is no known viral protein in this molecular weight range, the cross-linked product is transitory in nature and location specific and the cross-linking can be specifically inhibited by the WT peptide. These observations virtually rule out the possibility that Tin-2 is an artifactual product of the cross-linking reaction. Like Tin-1, the identity of Tin-2 is unclear but unlike Tin-1 its physiological relevance is not. Antibodies raised against the Golgi-associated proteins p200 (Narula et al., 1992) and p230 (Kooy et al., 1992) did not recognize Tin-2 (unpublished observations; the antibodies were kindly provided by K. Matlin and P. Gleeson, respectively).

Tin-3 and Tin-4 are found associated with VSV G only after the viral protein leaves the TGN, most likely at the cell surface. Since the polarized sorting is a TGN event, Tin-3 and Tin-4 are less likely to play a role in the basolateral sorting. In fact, the molecular weight of Tin-4 (~220–250 kD) and the observation that it is also cross-linked in the intact

cells (data not shown) suggest that this is a trimeric form of VSV G. Although the trimerization of VSV G occurs rapidly during transit from the ER to Golgi and is complete before the protein reaches the TGN, the cross-linked trimers (or Tin-4) are not detected in the TGN samples (Fig. 7 *A*). It is noteworthy that the luminal domain and not the cytosolic tail of VSV G is responsible for the trimerization of the protein (Doms et al., 1988). Thus, the lack of cross-linking of VSV G trimers (or Tin-4) in the TGN of the permeabilized cells confirms the view that in our system the cross-linking is restricted to the cytosolic side.

In summary, we have devised a SLO-permeabilized cell system to reconstitute multiple stages of polarized transport in MDCK cells. Using this system we have provided evidence for the presence of putative basolateral sorter and identified proteins that associate with the cytoplasmic tail of VSV G. One of these proteins, Tin-2, is likely to play a critical role in the sorting and transport of this basolateral protein. A direct demonstration of its function and the mechanism of action awaits its isolation and characterization.

We thank Dr. S. Bhakdi and U. Weller (University of Mainz, Mainz, Germany) for the generous supply of highly purified SLO without which this work would not have progressed. We thank H. Lane (Costar Corp.) for providing the filters, H. Virta for culturing MDCK cells and for the antibodies against VSV G and HA proteins, C. Frederiksen for the technical help, and B. Hoflack and R. Parton for critically reading the manuscript.

This work was supported by Deutsche Forschungsgemeinschaft SFB 352.

Received for publication 15 October 1993, and in revised form 17 March 1994.

References

Apodaca, G., B. Aroeti, K. Tang, and K. E. Mostov. 1991. Brefeldin-A inhibits the delivery of the polymeric immunoglobulin receptor to the basolateral surface of MDCK cells. *J. Biol. Chem.* 268:20380–20385.

Balch, W. E., W. G. Dunphy, W. A. Braell, and J. E. Rothman. 1984. Reconstitution of the transport of protein between successive compartments of the Golgi measured by the coupled incorporation of N-acetylglucosamine. *Cell.* 39:405–416.

Bennett, M., A. Wandinger-Ness, K. Simons. 1988. Release of putative exocytic transport vesicles from perforated MDCK cells. *EMBO (Eur. Mol. Biol. Organ.) J.* 7:4075–4085.

Bhakdi, S., and J. Tranum-Jensen. 1987. Damage to mammalian cells by proteins that form transmembrane pores. *Rev. Physiol. Biochem. Pharmacol.* 107:147–223.

Bhakdi, S., M. Roth, A. Sziegoleit, and J. Tranum-Jensen. 1984. Isolation and identification of two hemolytic forms of Streptolysin O. *Infect. Immunol.* 46:394–400.

Casanova, J. E., G. Apodaca, and K. E. Mostov. 1991. An autonomous signal for basolateral sorting in the cytoplasmic domain of the polymeric immunoglobulin receptor. *Cell.* 66:65–75.

Doms, R. W., A. Ruusala, C. Machamer, J. Helenius, A. Helenius, and J. K. Rose. 1988. Differential effects of mutations in three domains on folding, quaternary structure, and intracellular transport of vesicular stomatitis virus G protein. *J. Cell Biol.* 107:89–99.

Fuller, S. D., R. Bravo, and K. Simons. 1985. An enzymatic assay reveals that proteins destined for the apical and basolateral domains of an epithelial cell line share the same late Golgi compartments. *EMBO (Eur. Mol. Biol. Organ.) J.* 4:297–307.

Gomperts, B. D. 1990. GE: GTP-binding protein mediating exocytosis. *Annu. Rev. Physiol.* 52:591–606.

Gravotta, D., M. Adesnik, and D. Sabatini. 1990. Transport of influenza HA from the trans-Golgi network to the apical surface of MDCK cells permeabilized in their basolateral plasma membranes: energy dependence and involvement of GTP-binding proteins. *J. Cell Biol.* 111:2893–2908.

Griffiths, G., and K. Simons. 1986. The trans Golgi network: sorting at the exit site of the Golgi complex. *Science (Wash. DC).* 234:438–443.

Gruenberg, J., and K. Howell. 1989. Membrane traffic in endocytosis: Insights from cell-free assays. *Annu. Rev. Cell Biol.* 5:453–481.

Hunziker, W., C. Harter, K. Matter, and I. Mellman. 1991. Basolateral sorting in MDCK cells requires a distinct cytoplasmic domain determinant. *Cell.* 66:907–920.

Kobayashi, T., S. W. Pimplikar, R. G. Parton, S. Bhakdi, and K. Simons. 1992. Sphingolipid transport from the trans-Golgi network to the apical surface in permeabilized MDCK cells. *FEBS (Fed. Eur. Mol. Biochem. Soc.) Lett.* 300:227–231.

Kooy, J., B. Toh, J. M. Pettitt, R. Erlich, and P. A. Gleeson. 1992. Human autoantibodies as reagents to conserved Golgi compartments. Characterization of a peripheral, 230-kDa compartment-specific Golgi protein. *J. Biol. Chem.* 267:20255–20263.

Kreis, T. E., and H. F. Lodish. 1986. Oligomerization is essential for transport of vesicular stomatitis viral glycoprotein to the cell surface. *Cell.* 46: 929–937.

Laemmli, U. K. 1970. Cleavage of structural proteins during the assembly of the head of the bacteriophage T4. *Nature (Lond.).* 227:680–685.

Le Bivic, A., Y. Sambuy, A. Patzak, N. Patil, M. Chao, and E. Rodriguez-Boulan. 1991. An internal deletion in the cytoplasmic tail reverses the apical localization of human NGF receptor in transfected MDCK cells. *J. Cell Biol.* 115:607–618.

Lisanti, M. P., M. Sargiocomo, L. Graeve, A. R. Saltiel, and E. Rodriguez-Boulan. 1988. Polarized apical distribution of glycophosphatidylinositol-anchored proteins in a renal epithelial cell line. *Proc. Natl. Acad. Sci. USA.* 85:9557–9561.

Matlin, K. S., and K. Simons. 1983. Reduced temperature prevents transfer of a membrane glycoprotein to the cell surface but does not prevent terminal glycosylation. *Cell.* 34:233–243.

Matlin, K. S., and K. Simons. 1984. Sorting of an apical plasma membrane glycoprotein occurs before it reaches the cell surface in cultured epithelial cells. *J. Cell Biol.* 99:2131–2139.

Matlin, K. S., H. Reggio, A. Helenius, and K. Simons. 1981. Infectious entry pathway of influenza virus in a canine kidney cell line. *J. Cell Biol.* 91:601–613.

Matter, K., W. Hunziker, and I. Mellman. 1992. Basolateral sorting of LDL receptor in MDCK cells: the cytoplasmic domain contains two tyrosine-dependent targeting determinants. *Cell.* 71:741–753.

Mostov, K. E., G. Apodca, B. Aroeti, and C. Okamoto. 1992. Plasma membrane protein sorting in polarized epithelial cells. *J. Cell Biol.* 116:577–583.

Narula, N., I. McMarrow, G. Plopper, J. Doherty, K. S. Matlin, B. Burke, and J. Stow. 1992. Identification of a 200 kD Brefeldin-sensitive protein on Golgi membranes. *J. Cell Biol.* 117:27–38.

Pfeiffer, S., S. D Fuller, and K. Simons. 1985. Intracellular sorting and basolateral appearance of the G protein of vesicular stomatitis virus in Madin-Darby canine kidney cells. *J. Cell Biol.* 101:470–476.

Pimplikar, S. W., and K. Simons. 1993. Regulation of apical transport in epithelial cells by Gs class of heterotrimeric G protein. *Nature (Lond.).* 362: 456–458.

Prill, V., L. Lehmann, K. von Figura, and C. Peters. 1993. The cytoplasmic tail of lysosomal acid phosphatase contains overlapping but distinct signals for basolateral sorting and rapid internalization in polarized MDCK cells. *EMBO (Eur. Mol. Biol. Organ.) J.* 12:2181–2193.

Pryer, N. K., L. J. Wuesthube, and R. Schekman. 1992. Vesicle-mediated protein sorting. *Annu. Rev. Biochem.* 61:471–516.

Rindler, M. J., I. E. Ivanov, H. Plesken, E. Rodriguez-Boulan, and D. D. Sabatini. 1984. Viral glycoproteins destined for apical or basolateral plasma membrane domains traverse the same Golgi apparatus during their intracellular transport in doubly infected Madin-Darby canine kidney cells. *J. Cell Biol.* 98:1304–1319.

Rodriguez-Boulan, E., and S. K. Powell. 1992. Polarity of epithelial and neuronal cells. *Annu. Rev. Cell Biol.* 8:395–427.

Rothman, J. E., and L. Orci. 1992. Molecular dissection of the secretory pathway. *Nature (Lond.).* 355:409–415.

Simons, K., and H. Virta. 1987. Perforated MDCK cells support intracellular transport. *EMBO (Eur. Mol. Biol. Organ.) J.* 6:2241–2247.

Simons, K., and A. Wandinger-Ness. 1990. Polarized sorting in epithelia. *Cell.* 62:207–210.

Staros, J. V. 1982. N-Hydroxysulfosuccinimideactive esters: bis(N-hydroxysuccinimide) esters of two dicarboxylic acids are hydrophilic, membrane impermeant, protein cross-linkers. *Biochemistry.* 21:3950–3955.

Tan, A., J. Bolscher, C. Feltkamp, and H. Ploegh. 1992. Retrograde transport from the Golgi region to the endoplasmic reticulum is sensitive to GTPγS. *J. Cell Biol.* 116:1357–1367.

Thomas, D. C., C. B. Brewer, and M. G. Roth. 1993. Vesicular stomatitis virus glycoprotein contains a dominant cytoplasmic basolateral sorting signal critically dependent upon a tyrosine. *J. Biol. Chem.* 268:3313–3320.

Wandinger-Ness, A., M. K. Bennett, C. Antony, and K. Simons. 1990. Distinct transport vesicles mediate the delivery of plasma membrane proteins to the apical and basolateral domains of MDCK cells. *J. Cell Biol.* 111:987–1000.

Yokode, M., R. K. Pathak, R. E. Hammer, M. S. Brown, J. L. Goldstein, and R. G. W. Anderson. 1992. Cytoplasmic sequences required for basolateral targeting of LDL receptor in livers of transgenic mice. *J. Cell Biol.* 117:39–46.